www.czasopisma.pan.pl PAN www.journals.pan.pl

ARCHIVES of FOUNDRY ENGINEERING

ISSN (2299-2944)
Volume 18
Issue 1/2018

196 – 202

DOI: 10.24425/118837

36/1

Published quarterly as the organ of the Foundry Commission of the Polish Academy of Sciences

The Influence of Variable Parameters of Horizontal Continuous Casting on the Structure of AlCu4MgSi Alloy Ingots

P.M. Nuckowski [a, *], T. Wróbel [b]

[a] Institute of Engineering Materials and Biomaterials, Silesian University of Technology, Konarskiego 18A, 44-100 Gliwice, Poland

[b] Department of Foundry Engineering, Silesian University of Technology, Towarowa 7, 44-100 Gliwice, Poland

*Corresponding author. E-mail address: pawel.nuckowski@polsl.pl

Received 28.06.2017; accepted in revised form 29.07.2017

Abstract

The article presents results of research on the influence of variable parameters of horizontal continuous casting on the structure of AlCu4MgSi (EN AW-2017A) alloy ingots. The special character of the process allows for a continuous change of some of its parameters, namely, of the casting speed and of the rate of the cooling fluid flow thorough the crystallizer. These parameters have a significant impact on the crystallization process of the liquid metal. Depending on the cooling rate, intensity of the convection inside the solidifying alloy, and its chemical composition, there may arise some differences in the structure of the cast. In this study, ingots obtained at different casting speeds have been analyzed. The research methodology, based on light microscopy and electron microscopy (SEM), as well as energy dispersive spectroscopy (EDS) and X-ray diffraction (XRD), allowed for a thorough examination of the structure of the studied materials. The results were shown that an increase in the ingot casting speed leads to an increase in the average grain surface area.

Keywords: Metallography, Aluminum alloys, Horizontal continuous casting, Structure analysis, X-ray diffraction, Phase analysis

1. Introduction

Aluminum alloys, relative to the whole group of non-ferrous alloys, have wide-ranging industrial applications. There has been a steady growth in the demand for aluminum alloy goods, which, whether in the form of finished products, intermediate products or raw materials, find use in different branches of economy, such as the automotive, aerospace, chemical, construction, and energy industries. Aluminum owes its high popularity to its low density, equal to 2.6989 g/cm3 at 293 K, due to which structures made out of its alloys have lower proper mass than steel structures, while maintaining an optimal mass to strength ratio. The ability of aluminum and its alloys to undergo passivation provides significant corrosion resistance in pH 4–9 environments, which increases the lifespan of aluminum structures and their elements [1-4].

Due to their good castability and low casting contraction, aluminum alloys make good casting materials. Aluminum casts can be obtained using most of the known casting methods, including lost-wax casting, gravity die casting, centrifugal casting, low- and high-pressure casting, as well as continuous and semi-continuous casting [5-8]. In the process of continuous casting, the ingot is obtained by means of a controlled flow of molten metal between the crystallizer walls. The flowing metal, due to heat dissipation through the walls, changes its physical state from liquid to solid, while maintaining the shape of the crystallizer. The ingot can be cut into pieces of desired lengths. This method, due

to its high efficiency and the possibility to integrate it with processes of plastic working, is finding growing applications in the industries oriented on processing aluminum alloys intended for plastic working. Apart from cost reduction, coming from lowering energy consumption, and the decrease in the amount of waste, one of the most important factors in considering the continuous casting process is the possibility to affect the structure of the cast metal [6, 9, 10]. The run of the crystallization process, following the pouring of the molten metal into the mold, affects the forming of the primary structure of the cast, which, in turn, directly determines the physical and technological properties of the material [9-11]. Moreover, the process of continuous casting, in addition to aluminum alloys, it is also used to production of ingots of other non-ferrous metals, such as copper [12-13] and magnesium [14].

2. Description of research

The special character of the continuous casting process allows for varying some of its parameters, namely, the casting speed and the rate of the cooling liquid flow through the crystallizer. These parameters have a significant influence on the course of the crystallization process of the liquid metal. Depending on the cooling rate, the intensity of the convection currents inside the solidifying alloy, and its chemical composition, there will be differences in the structure of the cast.

This article presents results of research on the impact of changes of crystallization conditions in the process of continuous casting of EN AW-2017A aluminum alloy on the formation of its structure.

3. Material and methodology

In this experiment, 30mm-diameter ingots (Fig.1) were made, using a horizontal continuous casting test stand (Fig. 2), out of AlCu4MgSi (EN AW-2017A) alloy, the chemical composition of which is shown in Table 1.

The cast was made using the method of intermittent ingot extraction: "forward step – pause", with the pause time (t_p) to step time (t_s) ratio of 1:2, which, at the instantaneous forward motion speed V_m staying in the range 100 to 300 mm/min, allowed for an average casting speed V_a in the range 30 to 100 mm/min, with the cooling water flow rate Q being in the range 0.5 to 1.2 l/min. Depending on the used casting speed the temperature of the cooling water T_w was in the range 45÷55 ^oC, and the temperature of the ingot T_i after leaving the crystallizer was equal to 150÷300 ^oC. The parameters of the process of horizontal casting of EN AW-2017A alloy ingot are presented in Table 2.

Before metallographic testing, preliminarily ground ingot fragments were polished on felt polishing wheels with the use of diamond suspensions with particle sizes of 6 and 3 µm, and an OP-U suspension. For the purposes of polarized light observations, the specimens were electrolytically etched in an aqueous solution of tetrafluoroboric acid.

Table 1.
Chemical composition of EN AW-2017A alloy

Alloy	Mass concentration [% wt]								
	Si	Fe	Cu	Mn	Mg	Cr	Zn	other	Al
EN AW-2107A	0,2 ÷ 0,8	≤ 0,7	3,5 ÷ 4,5	0,4 ÷ 1,0	0,4 ÷ 1,0	≤ 0,1	≤ 0,25	≤ 0,15 (total)	rest
note: Zr+Ti ≤0,25									

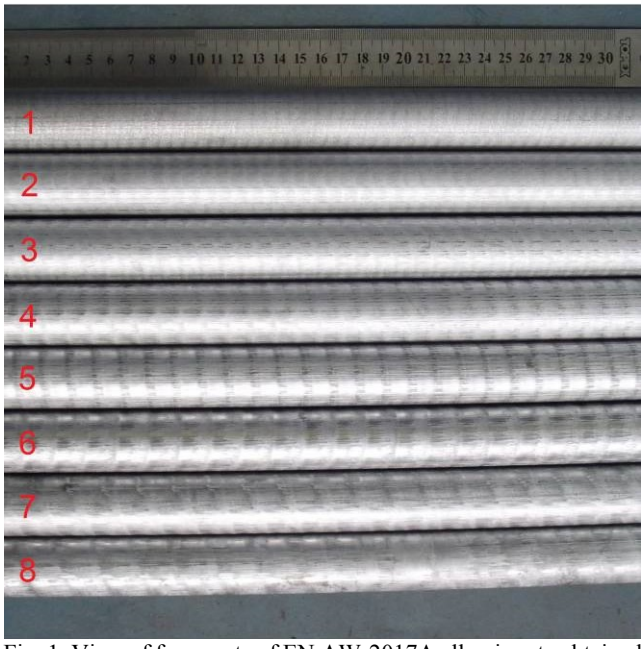

Fig. 1. View of fragments of EN AW-2017A alloy ingots obtained in the process of horizontal continuous casting

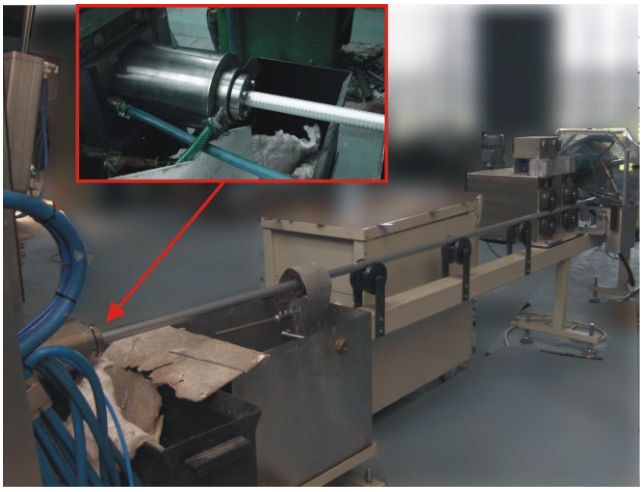
Fig. 2. View of stand of horizontal continuous casting

Table 2.
Parameters of horizontal continuous casting of EN AW-2017A alloy ingots

Mark of ingot	t_p [s]	t_s [s]	V_m [mm/min]	V_a [mm/min]	Q [l/min]	T_w [°C]	T_i [°C]
1	1	2	100	30	0,5	45 ÷ 55	150
2	1	2	120	40	0,7		170
3	1	2	150	50	0,9		190
4	1	2	180	60	0,9		210
5	1	2	210	70	1,0		230
6	1	2	240	80	1,2		250
7	1	2	270	90	1,2		270
8	1	2	300	100	1,2		300

The photographs of the structure of the examined ingots were made using a Zeiss Axio Observer light microscope, utilizing bright-field and polarized-light observation techniques.

The number of grains and their averaged surface area in planar ingot cross-sections were determined, based on the Jeffries method, using the ImageJ image analysis software.

The analysis of the chemical composition of the structure elements in microregions was performed with the use of a Phenom ProX scanning microscope, equipped with an energy dispersive X-ray spectrometer (EDS).

The ingot phase composition has been determined on the basis of the X-ray diffraction measurements, performed with the use of Panalytical X'Pert Pro MPD diffractometer, utilizing filtered radiation of a cobalt-anode lamp ($\lambda K\alpha$= 0.179 nm). The diffraction lines were recorded, using the step-scanning method [15] in the Bragg – Brentano geometry, by means of a PIXcell 3D detector, placed on the diffracted beam axis, in the angle range from 20–120° [2θ] (1 step = 0.03°, count time per step = 80s). The obtained diffractograms were analyzed with the help of Panalytical High Score Plus software, together with the PAN-ICSD structure database. Hardness test was performed on the ingots using a Zwick ZHR hardness tester.

4. Results and discussion

To determine the influence of variable parameters of horizontal continuous casting on the structure of EN AW-2017A alloy, eight ingot fragments (Fig.1), obtained at different casting speeds, were analyzed. Characteristic "bands", being traces of ingot rest stops inside the crystallizer during cyclic "forward step – pause" movement, were observed on the surface of all ingots. The distances between the bands on the ingot surface decrease as the average casting speed increases, and their presence does affect in any significant way the surface quality.

Metallographic studies (Fig.3–Fig.8) of cross-sections of ingots that were obtained in the process of continuous casting showed that the structure comprises mainly of equiaxed grains, of irregular shapes and various dimensions. The visible contrast in grain coloration, revealed in polarized light observations, is a consequence of different crystallographic orientations of the grains. A low number of small equiaxed grains, the so called chill crystals, located in the outer ingot zone, has also been observed. On the basis of the analysis of the average grain surface area (table 3), it has been established, that as the ingot casting speed increases, the average grain size increases too. For the ingot cast with a speed of 30 mm/min, the averaged grain surface area was equal to 0.037 mm2. In the case of the ingot cast with a speed of 100 mm/min, the grain surface area increased to 0.1 mm2, approximately. This relationship is closely connected with the cooling rate, which decreases as the casting speed increases. Based on the information in literature [16, 17], it can be inferred that an increase in the cooling rate leads to an increase in the solid solution nucleation temperature α. This phenomenon is related to a formation of fluctuating clusters or embryos, which under conditions of significant supercooling may play the role of nucleation pads, which directly influences the grain size.

Table 3.
Results of analysis of average grain area

Average casting speed V_a[mm/min]	Number of grains in the counting area	Average value of grain surface area [mm^2]
30	116,25	0,037
40	78,50	0,055
50	71,75	0,060
60	67,25	0,064
70	59,75	0,072
80	53,75	0,080
90	46,25	0,093
100	41,75	0,103

To determine the type and morphology of non-equilibrium phase precipitates in the structure of analyzed ingots, SEM observations and chemical analysis in microregions, by means of energy dispersive X-ray spectroscopy (EDS), were performed.

The analyzed materials are characterized by dendritic structure. In the interdendritic regions, a lattice of eutectic precipitates, as well as isolated precipitates of non-equilibrium phases (Fig.9 and 10), have been observed. It has been determined that their morphology depends on the ingot casting speed. As the casting speed increases, the fraction of globular precipitates decreases, and the shape of the lattice formed by precipitates of non-equilibrium phases changes.

An analysis performed with the use of an EDS detector has shown significant variation of chemical composition in the precipitate regions (Fig.11, Tab.4). This heterogeneity can be also observed, as a variation in contrast, in the photographs of the structure of the analyzed materials, obtained with the help of an SE detector. Based on the performed analysis, and on literature [18-21], it can be hypothesized that the bright precipitate regions (white areas, in the precipitate marked with points 4, 5, 7 and 8), containing aluminum and copper, are the θ-Al_2Cu intermetallic phase. Also, the observed dark, punctual, magnesium and silicon-rich precipitates (black areas, in the precipitate marked with points 4 and 5) are probably the β-Mg_2Si phase (Fig.12). The areas appearing as gray can be, on the other hand, connected to $Al_{X1}Si_{X2}Mn_{X3}Fe_{X4}Cu_{X5}$ and $Al_{X1}Cu_{X2}Mg_{X3}Si_{X4}$ complex intermetallic phases. Finally, acicular precipitates of eutectic silicon were identified in the analyzed structure, too.

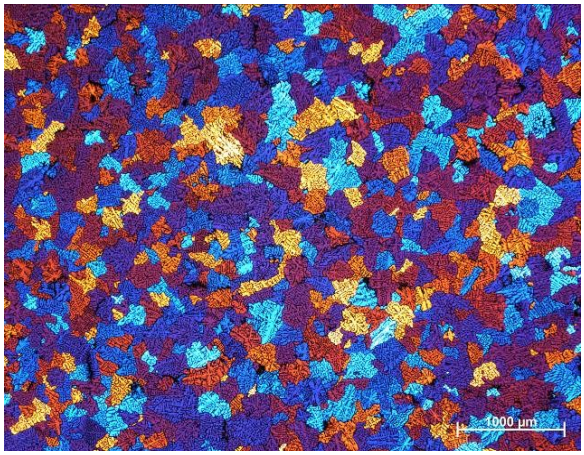

Fig. 3. Structure of the ingot cast with an average speed of V_a = 30 mm/min; cross-section – middle part (light microscope, polarized light)

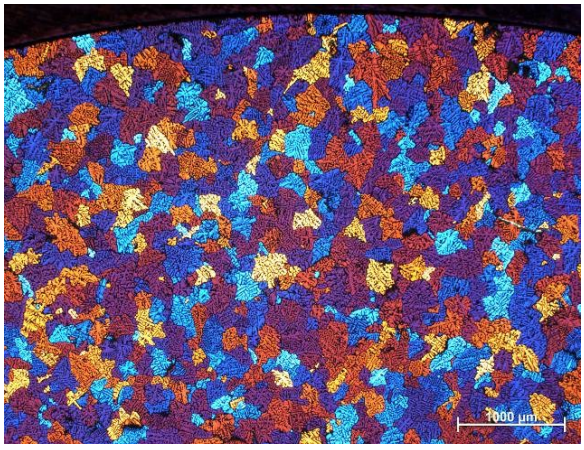

Fig. 4. Structure of the ingot cast with an average speed of V_a = 30 mm/min; cross-section – outer part (light microscope, polarized light)

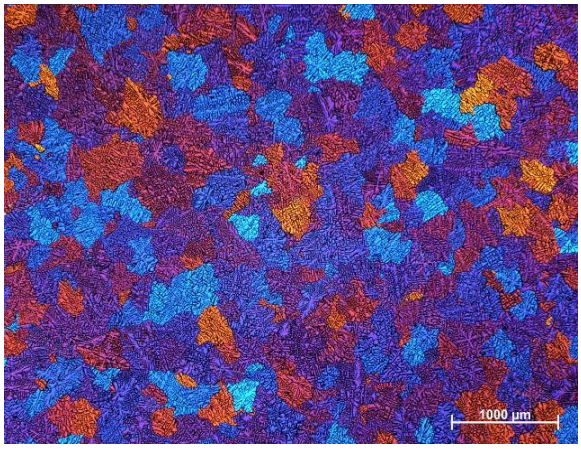

Fig. 5. Structure of the ingot cast with an average speed of V_a = 60 mm/min; cross-section – middle part (light microscope, polarized light)

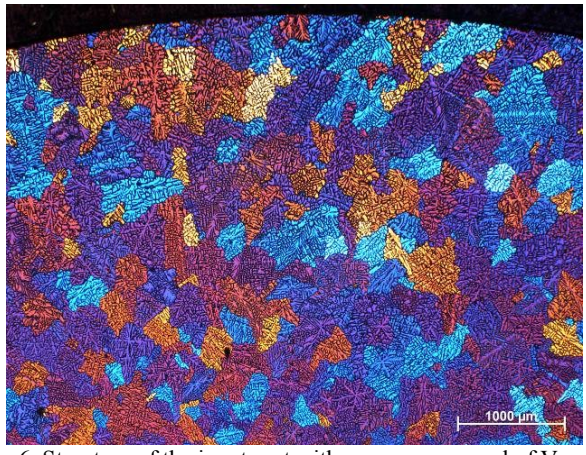

Fig. 6. Structure of the ingot cast with an average speed of V_a = 60 mm/min; cross-section – outer part (light microscope, polarized light)

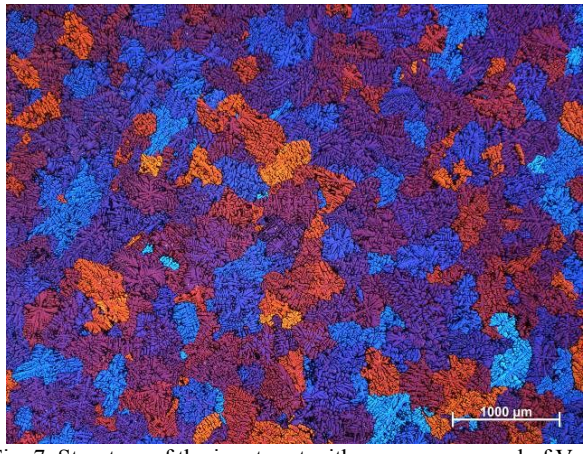

Fig. 7. Structure of the ingot cast with an average speed of V_a = 100 mm/min; cross-section – middle part (light microscope, polarized light)

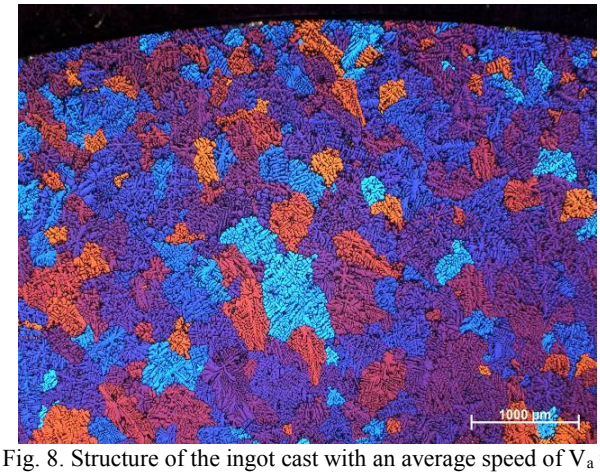

Fig. 8. Structure of the ingot cast with an average speed of V_a = 100 mm/min; cross-section – outer part (light microscope, polarized light)

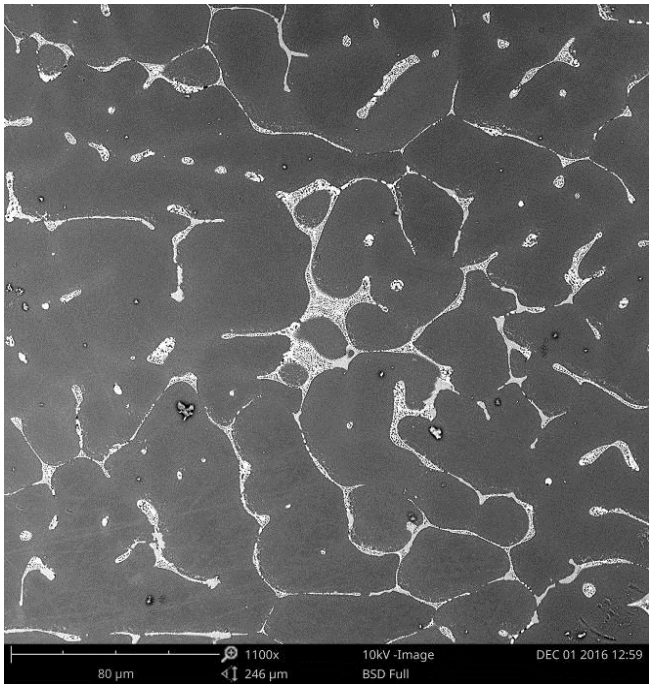

Fig. 9. Structure of the ingot cast with an average speed of V_a = 30 mm/min; cross-section (SEM)

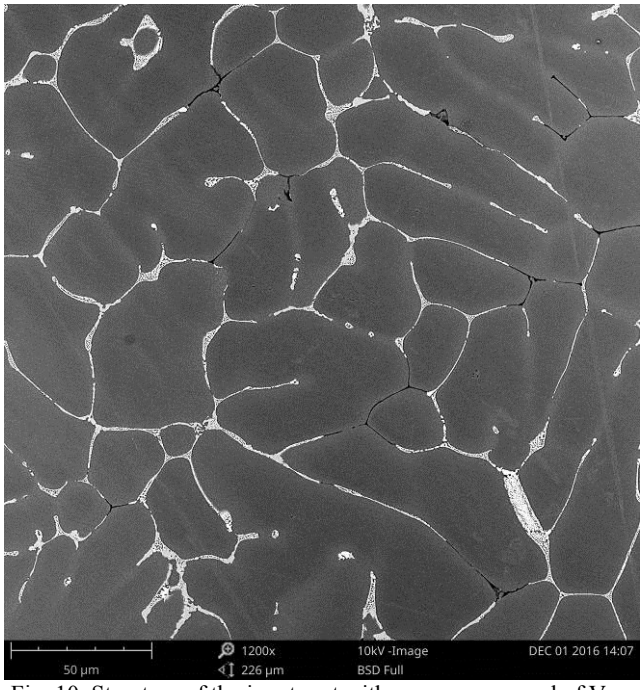

Fig. 10. Structure of the ingot cast with an average speed of V_a = 100 mm/min; cross-section (SEM)

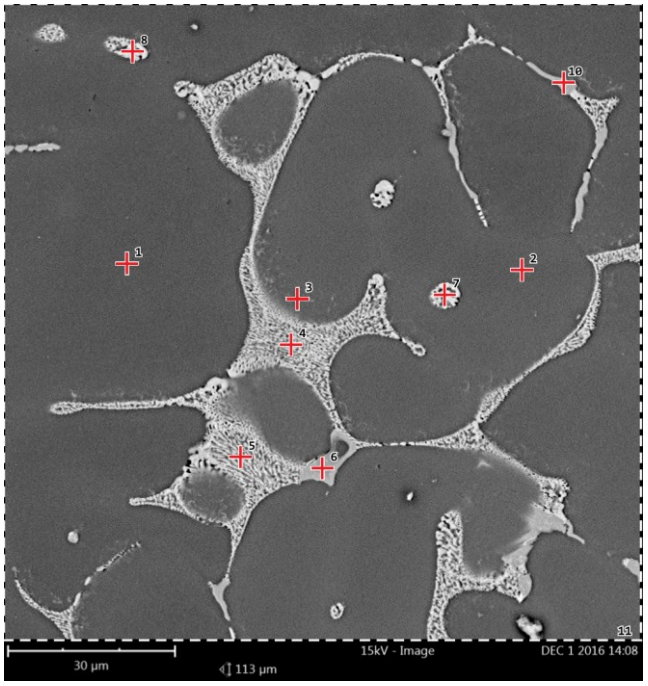

Fig. 11. Structure of the ingot cast with an average speed of V_a = 30 mm/min; cross-section (SEM)

Fig. 12. Morphology of precipitates of non-equilibrium phases in the structure of ingot pulled with an average speed of V_a = 30 mm/min; cross-section (SEM)

Table 4.
Results of chemical composition analysis in microregions of analyzed samples (SEM – EDS)

Place of analysis (Fig.11)	Atomic concentration [%]					
	Al	Cu	Mg	Si	Fe	Mn
1	≈99	-	-	-	-	-
2	≈99	-	-	-	-	-
3	97,7	2,3	-	-	-	-
4	79,2	13,9	3,9	2,9	-	-
5	76,3	15,6	5,0	3,1	-	-
6	84,4	3,9	-	5.0	3,7	3,1
7	78.6	21,4	-	-	-	-
8	77,7	22,3	-	-	-	-
10	78,2	4,2	-	6,8	5,9	4,8
11 map	94,7	2,7	1,6	0,6	0,1	0,3

The results of X-ray diffraction qualitative phase analysis (Fig.13) confirmed the presence of an α-Al solid solution, as well as the θ-Al_2Cu and β-Mg_2Si intermetallic phases. The analyzed diffractograms did not show diffraction lines connected to $Al_{X1}Si_{X2}Mn_{X3}Fe_{X4}Cu_{X5}$ and $Al_{X1}Cu_{X2}Mg_{X3}Si_{X4}$ complex intermetallic phases. It can be speculated that the volume fraction of these phases lies below the method limit sensitivity. To determine the volume fraction of the identified phases, an X-ray diffraction quantitative phase analysis has been performed, using the least squares method (Rietveld refinement). On the basis of the obtained results (table 5), it has been determined that, in the precipitation areas, the biggest fraction is that of the θ-Al_2Cu intermetallic phase (2.5 – 4% by volume, approx.). The volume fraction of the β-Mg_2Si phase is no greater than 1%.

The results of hardness test (Fig. 14), showed that the change of casting speed does not significantly affect to the hardness of the ingots.

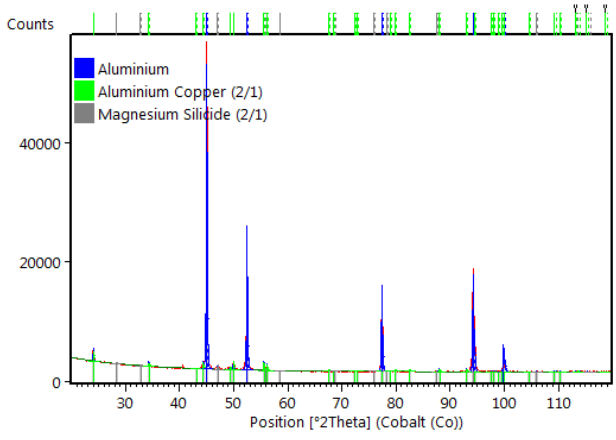

Fig. 13. Diffraction pattern obtained for sample from the ingot cast with an average speed of V_a = 60 mm/min

Table 5.
Percentage fraction of identified crystalline phase in the analyzed AlCu4MgSi alloy (Rietveld method)

Average casting speed V_a [mm/min]	Fraction of crystalline phase [% vol.]		
	α-Al	θ-Al_2Cu	β-Mg_2Si
30	95,9	3,5	0,6
40	96,9	2,5	0,5
50	95,9	3,4	0,7
60	95,1	4,1	0,8
70	96,3	3,1	0,6
80	97,2	2,4	0,5
90	95,7	3,6	0,7
100	95,1	4,0	0,9

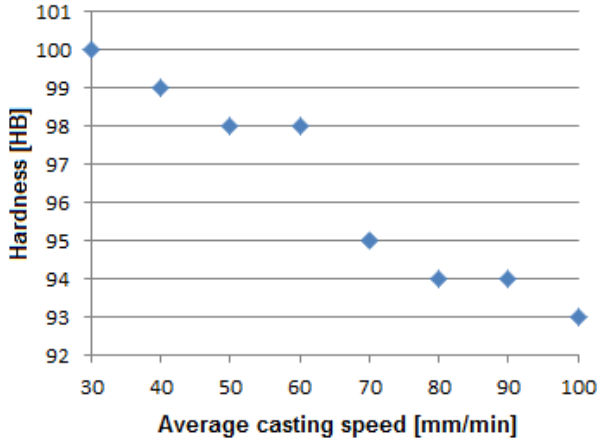

Fig. 14. Results of hardness test of the ingots obtained in different casting speeds

5. Conclusions

The results of this study allowed us to determine the influence of the parameters of the continuous casting process on the AlCu4MgSi (EN AW-2017A) alloy ingot structure.

It was shown that an increase in the ingot casting speed leads to an increase in the averaged grain surface area, due to a reduced temperature gradient at the crystallization front. This dependence is closely related to the cooling rate, which decreases as the ingot casting speed increases. Regardless of the process parameters, it is mainly equiaxed grains that occur in the structure of the obtained ingots. Changing the parameters of the continuous casting process also affects the shape and morphology of the precipitates of non-equilibrium phases predominantly θ-Al_2Cu and β-Mg_2Si, located mainly in interdendritic regions.

Qualitative and quantitative X-ray diffraction phase analysis of the samples taken from ingots confirmed that those precipitates were mainly composed of the θ-Al_2Cu and β-Mg_2Si intermetallic phases.

References

[1] Kvačkaj, T., Bidulskỳ, R. (ed.). (2011). *Aluminium Alloys, Theory and Applications*. Rijeka: InTech.

[2] Zaki, A. (ed.). (2012). *Aluminium Alloys – New Trends in Fabrication and Applications*. Rijeka: InTech.

[3] Dobrzański, L.A., Macek, M., Tomiczek, B., Nuckowski, P.M., Nowak, A.J. (2016). The influence of the dispersion method on the microstructure and properties of MWCNTs/AA6061 composites. *Archives of Metallurgy and Materials*. 61(2), 1229-1234.

[4] Szklarska-Smialowska, Z. (1999). Pitting corrosion of aluminium. *Corrosion Science.* 41, 1743-1767.

[5] Polmear, I., St. John, D., Nie, J-F., Qian, M. (2017). *Light Alloys* (fifth ed.). Cambridge: Elsevier Ltd.

[6] Wróbel, T., Szajnar, J., Bartocha, D., Stawarz, M. (2017). Primary Structure and Mechanical Properties of AlSi2 Alloy Continuous Ingots. *Archives of Foundry Engineering*. 17(2), 145-150.

[7] Szajnar, J., Wróbel, T., Bartocha, D., Stawarz M. (2016). Inoculation of Al-Si alloys using the electromagnetic stirring method. *Transactions of Foundry Research Institute.* 56(2), 67-75 (in Polish)

[8] Wróbel, T., Szajnar, J. (2013). Horizontal continuous casting of Al and Al-Si Alloy in semi-industrial conditions. In 22nd International Conference on Metallurgy and Materials: METAL 2013, 15-17 May 2013 (pp. 1177-1182). Brno, Czech Republic: Tanger Ltd.

[9] Schrewe, H. F. (1991). *Continuous Casting of Steel, Fundamental Principles and Practice.* Dusseldorf: Stahl und Eisen.

[10] Sebzda, W., Szajnar, J. (2013). Technological parameters influence on continuous cast grey iron. In 22nd International Conference on Metallurgy and Materials: METAL 2013, 15-17 May 2013 (pp. 178-184). Brno, Czech Republic: Tanger Ltd.

[11] Szajnar, J., Walasek, A., Baron, C. (2013). The description of the mechanism for the alloy layer forming process based on the experimental examination. In 22nd International Conference on Metallurgy and Materials: METAL 2013, 15-17 May 2013 (pp. 134-139). Brno, Czech Republic: Tanger Ltd.

[12] Yan, Z., Jin, W., Li, T. (2012). Effect of rotating magnetic field (RMF) on segregation of solute elements in CuNi10Fe1Mn alloy hollow billet. *Journal of Materials Engineering and Performance*. 21(9), 1970-1977.

[13] Li, X., Guo, Z., Zhao, X., Wie, B., Chen, F., Li, T. (2007). Continuous casting of copper tube billets under rotating electromagnetic field. *Materials Science & Engineering A*. 460-461, 648-651

[14] Okayasu, M., Wu, S., Tanimoto, T., Takeuchi, S. (2016). Mechanical Properties of Magnesium AlloysbProduced by the Heated Mold Continuous Casting Process. *Archives of Foundry Engineering*. 16(4), 208-216.

[15] Grajcar, A., Kwaśny, W., Zalecki, W. (2015). Microstructure-property relationships in TRIP aided medium-C bainitic steel with lamellar retained austenite. *Materials Science and Technology*. 31(7), 781-794.

[16] Dobrzański, L.A., Maniara, R., Sokolowski, J. (2006). Kinetics of crystallization and structure of AC AlSi7Cu4 foundry alloy. *Archives of Foundry*. 6(21), 125-132 (in Polish).

[17] Fraś, E. (2003). *Crystallization of metals*. Warszawa: WNT. (in Polish).

[18] Chakrabarti, D.J., Laughlin, D.E. (2004). Phase relations and precipitation in Al-Mg-Si alloys with Cu additions. *Progress in Materials Science*. 49, 389-410.

[19] Wierzbicka, B. (1998). Crystallization of Al-Cu alloys during the rapid cooling process. *Solidification of Metals and Alloys*. 38, 143-150.

[20] Riontino, G., Zanada, A. (1998). Coupled formation of hardening particles on pre-precipitates in an Al–Cu–Mg–Si 2014 alloy. *Materials Letters*. 37(4-5), (241-245).

[21] Totten, G. E., MacKenzie, D. S. (ed.) (2003). *Handbook of Aluminum volume 1 Physical Metallurgy and Processes*. New York: Marcel Dekker Inc.